AFCI Quarterly Input – UNLV
January through March, 2004

1.0 University of Nevada, Las Vegas (UNLV)

UNLV Transmutation Research Program. The University of Nevada, Las Vegas supports the AFCI through research and development of technologies for economic and environmentally sound refinement of spent nuclear fuel. The UNLV program has four components: infrastructure, international collaboration, student-based research, and management and program support.

- Six students and one staff from UNLV attended the MCNPX introductory training workshop at UNLV held January 12-16.
- Thirteen proposals for graduate student research starting summer term 2004 were submitted to the DOE Program Advisory Committee. The top three ranked new proposals and three proposals on continuing projects were approved by the UNLV Finance Committee.

1.1 Infrastructure Augmentation

1.1.1 Infrastructure Augmentation Scope

The infrastructure augmentation component of the UNLV Transmutation Research Program enhances UNLV's research staff, facilities, and academic programs to increase the ability of the university to perform AFCI research.

1.1.2 Infrastructure Augmentation Highlights

- **Ph.D. Program in Radiochemistry**. The proposed Ph.D. program in Radiochemistry was approved March 19 by the University and Community College System of Nevada Board of Regents. The program will be offered Fall term 2004. The program will be a joint program between the Department of Chemistry and the Department of Health Physics and will be governed by the Graduate College.

- **Facilities Progress Update**. The Transmission Electron Microscope was officially accepted by UNLV from the FEI vendor. An acoustic vibration mitigation system still needs to be added in order for the TEM to be meet its full capability. However, the system is now usable. Two other facilities, the Inductively Coupled Plasma Atomic Emission Spectrometer user facility and an interim Actinide Chemistry laboratory are under remodel as a dedicated ventilation system has been designed and will be completed next quarter.

1.2 International Collaboration

1.2.1 International Collaboration Scope

The international collaboration component of the UNLV Transmutation Research Program enhances UNLV's breadth of scientific and scholastic experience. University collaboration is also an efficient conduit for international collaboration that benefits the national AFCI program. UNLV has ongoing relationships with the Khlopin Radium Institute (KRI) in St. Petersburg, Russia; the Institute for Physics and Power Engineering (IPPE) in Obninsk, Russia; and members

of the International Molten Metal Advisory Committee (from Sweden, Germany, Belgium, and Italy).

1.2.2 International Collaboration Highlights

- **Khlopin Radium Institute**. Two final reports were submitted entitled "Development, Fabrication and Study of Fullerene-Containing Carbon Material (FCC) for Immobilization of Iodine" and "Development of Fluorapatite as a Waste Form" for first-year activities for Tasks 15 and 16, respectively.

1.3 Student Research

1.3.1 Student Research Scope

The Student Research component is the core of the UNLV Transmutation Research Program with steadily increasing funds as the program evolves and capability expands. The milestones, schedules, and deliverables of the student research projects are detailed in the individual research proposals. UNLV currently has 16 student research tasks that include 37 graduate students and involve 28 faculty members. The tasks are divided below in terms of their research area: fuels, separations, and transmutation sciences.

1.3.2 Student Research Highlights

FUELS TECHNOLOGY

Metallic Fuel Pins (Task 1) Highlights.

- Four different power output rates varying from 100% to 25% of given frequency 6400 Hz are simulated in order to check its influence on the induction heating process based on ANL's system.
- The frequency of the current has a great impact on the induction heating process. A high frequency, greater than 1600 Hz, is needed to reach the melting point within a short time. Also, one can control the melting process by controlling the frequency.
- The comparison of the simulations of the case considering the latent heat and the case without considering the latent heat was completed. Since the induction melting system has a very high power, the latent heat is relatively small compared to the heat deposited in the feedstock. So there is only a small difference between the two temperature values. The study case considering latent heat has a lower temperature and takes a little longer time to reach the maximum temperature.
- The "slope" method was used to try to solve the system model. The methodology works well for the energy equations, but not for the momentum equations and continuity equation. The CFD case diverged when the calculated temperature approached the melting point of material. Work continues to evaluate different calculation methods to couple the phase change problem.

Remote Fuel Fabrication (Task 9) Highlights.

- Development of operating/control of the Hot Cell robotic assembly continued. The Pick and place dynamic simulation, including feedback control with Matlab has been developed and is now incorporated in the control simulation.

- The engineering college upgraded the ProEngineer CAD software. Unfortunately, there seem to be compatibility issues with Visual Nastran, which is central to our hot cell simulations. The software vendors concerned were contacted regarding solutions/patches to resolve this problem.

SEPARATIONS TECHNOLOGY

Systems Engineering Model (Task 8) Highlights.

- The general-purpose design of the system engineering model has been created. One key component that separates the developed software of TRPSEMPro from the existing AMUSE is its scalability and extensibility. The system creates a mid-ware, called AMUSESimulator, that connects between Argonne's AMUSE macros and the main TRPSEMPro. Such module designs later will be used to connect all the outside modules provided by Argonne National Laboratory or other laboratories.
- Since the sensitive nature of the AMUSE code, the NCACM will not have the "correct" D-value through the calculation. The TRPSEMPro code can only be tested through some known case studies. In the future, ANL will need to bring back the package and install it on their system using the "actual" AMUSE code. Some system configuration assistance will be needed through the NCACM.
- As currently designed, the interface stores all data using MS SQL Server, an industrial standard for data storage. To simplify the use of the system/interface on personal computers at the national laboratories, as well as to increase the utility of the generated data, it has been decided to rework the interface to use a smaller database manager, such as MS ACCESS, to archive the data.

Criticality and Heat Transfer Analyses of Separations Processes (Task 11) Highlights.

- Meeting was held with Dr. James Laidler of Argonne National Lab and Yue Guan of AdSTM to discuss the systems engineering project which will link together work being done at ANL and UNLV as the basis for a new Ph.D. project as a follow on to the recently completed M.S. project.

Immobilization of Fission Iodine (Task 15) Highlights.

- Experiments were continued with FCC and NOM scavenging of iodine during simulated fuel dissolution. The formation of iodate was explored as a result of exposure to NOx and nitric acid. There are distinct differences between the iodine generator and the fuel rod simulator.
- Continuing to investigate and quantify the release of methyl iodide from iodine treated NOM.
- Some additional experiments were performed on measuring iodine reaction kinetics with NOM in aqueous suspensions.
- Experiments continued on recovery of iodide from the fuel rod simulator. It was discovered that iodine recoveries from the fuel rod simulation experiments are significantly less than quantitative.

- Variable temperature pyrolysis experiments of iodide loaded anion exchange resins were performed.

Fluorapatite Waste Forms (Task 16) Highlights.

- Developed techniques for Atomic Absorbtion Spectroscopy (AAS) to do the element analysis of samples.
- Synthesized Fluorapatite solid sample (received from Russia) was refluxed in Strontium Chloride solutions (in two different concentrations) for 6 hours.
- 5 samples of hydroxyapatites (with and without Zn) have been prepared. Obtained the SEM micrographs, EDS, XPS and FTIR spectra for these samples.
- Hydroxyl apatite mixed with Strontium Chloride and Calcium Fluoride were kept in aqueous medium in a round bottom flask for one week and two weeks. SEM data shows structural changes in Hydroxyl apatite. However, IR data shows apatite function groups are remaining unchanged.
- Another sample of Hydroxyl apatite was refluxed for seven hours with Sodium Fluoride and Strontium Nitrate. This time NaF was used instead of CaF_2 because it is more difficult to remove the less soluble CaF_2 form that has been used in previous refluxed mixtures.
- Elemental analysis of first 4 synthesized fluorapatite samples (using refluxing method) was done using Atomic Absorption Spectroscopy (AAS).
- For comparison, a second sample was prepared without refluxing. This sample was also analyzed by SEM, EDS and XPS before dissolution.
- Data analysis completed for almost all the samples that were synthesized.
- Two different refluxes were performed and samples of Sr-containing Fluorapatite were synthesized.
    - First Sample: Refluxed 1:2 (Hydroxyapatite to Strontium Chloride) while stirring for 24 hours (aqueous medium)
    - Second Sample: Refluxed 1:2 (Hap to Strontium Nitrate Solution) and for 27 hours. And kept the sample at room temperature for another 20 hours.
- Both samples were dried in the vacuum and in a desiccator and analyzed using SEM and IR spectroscopy. Only the second sample showed changes in both SEM data and in IR spectra.

TRANSMUTATION SCIENCES

Niobium Cavity Fabrication Optimization (Task 2) Highlights.

- LANL has supplied UNLV with surface conditioned Nb samples and raw Nb rod of the grade used in building their chambers
- Monte Carlo Back Scattering and Secondary Electron Scattering code is being modified to account for surface layer contamination. One portion of the Monte Carlo Back Scattering and Secondary Electron Scattering code has been verified against experimental work for 5 keV primary electrons. Code agreement for lower energy electrons is under investigation.
- Due to large potential gradients at the MCP and the detail design of the electron position detector, more exact particle trajectory calculations had to be performed which led to a slight modification in the overall design.

- The detector vendor is building a special accelerator tube with proper insulation to hold off high potentials. The presence of the tube will not affect the primary and secondary electrons beam dynamics.
- Assembly of multipacting experimental system continued:
    - Cleaned and assembled vacuum chamber, manipulator, pumps, and cryostat.
    - Currently working on verifying vacuum integrity.
    - Electron position detector arrived.

LBE Corrosion of Steel (Task 3) Highlights.

- Preliminary SEM and EDX data was collected on iron-silica alloys as part of collaboration with Eric Loewen, scientist at INEEL.
- Raman spectroscopy studies of the corrosion products were performed. Raman spectra for powder standards of Fe2O3, Fe3O4, and Cr were obtained. However, obtaining Raman spectrum of the corroded samples has proved difficult and is still under investigation.
- Planning and development of the drawings for the small experiments facility continued.

Environment-induced Degradation of Materials (Task 4) Highlights:

- Exposure experiments in the molten LBE using C-ring and U-bend specimens continued in LANL's Delta Loop. Specimens were also tested in high-temperature aqueous solutions for different exposure periods.
- Stress corrosion cracking (SCC) tests using smooth and notched tensile specimens of Alloys EP-823, HT-9 and 422 were performed under controlled electrochemical potential (E_{cont}) using both constant-load and slow-strain-rate testing techniques.
- Localized corrosion (pitting and crevice) studies were performed at ambient and elevated temperatures to evaluate the critical potentials in different solutions.
- Fractographic evaluations by scanning electron microscopy and microstructural analyses by optical microscopy were performed.

LBE Corrosion Modeling (Task 5) Highlights:

- 3-D simulation results for thermalhydraulics/wall concentration gradients of corrosion/precipitation in several LBE loop fittings was completed.
- How to better characterize the correlated results of increased wall concentration gradients at elbows to what has been hypothesized is due to increased secondary flows in these elbows was investigated. The procedure is to numerically calculate the "circulation strength" for different elbow sections and see how its trends develop downstream along the elbow.
- Completed grid independency study for the 3-D sudden expansion flow simulations for the different Reynolds numbers. Analytical models predict vortex shedding occurs at Re = 1500.
- Work to solve the Re=200,000 case with a different solver within STAR-CD was performed, with the primary concern being technical difficulties in linking the solvers.
- The velocity data generated from STAR-CD and the circulation theorem is being used to calculate the magnitude of circulation along four elbows of the loop.

Neutron Multiplicity Measurements of AAA Target/Blanket Materials (Task 6) Highlights:

- Denis Beller took over as the principal investigator on this task due to the departure of the former PI.
- The project scope was modified to focus on the careful documentation and use of the Russian-built Neutron Multiplicity Measurement System, which consists of a lead target, a polythene moderator, 64 ^{3}He detectors, the associated electronics, and a data acquisition and analysis system. The system will be used to measure neutron multiplicity in several accelerator-generated neutron environments, from a few to 800 MeV.
- Documentation was assembled in the form of a user guide including a physical description of the Neutron Multiplicity Detector System (NMDS), plans, drawings, operating instructions, calibration and measurement instructions, computer software for analysis, etc.
- Long-term background counts were acquired to examine neutron multiplicity from cosmic particles (e.g. muons).

Dose Conversion Coefficients (Task 7) Highlights:

- Dose coefficients for Category 2 radionuclides were reviewed and separated into a missing data and a complete data list. Category 2 radionuclides missing data were research and moved to Category 3 or had DC values calculated.
- DC's with complete data sets have been calculated by one of the three independent groups working on this project.

Properties of Alloy EP-823 (Task 10) Highlights:

- Mechanical testing of Alloys EP-823, HT-9 and 422 was performed at elevated temperatures in the presence of nitrogen.
- Some of the tested specimens were sectioned to prepare thin samples for evaluation of defects/dislocations by transmission electron microscopy (TEM).
- Additional tensile test specimens are being machined to study the effect of tempering time on deformation at elevated temperatures.
- Metallography and fractography are in progress involving all tested tensile specimens using optical microscopy and scanning electron microscopy, respectively.

Radiation Transport Modeling using Parallel Computational Techniques (Task 12) Highlights:

- Extensive studies on how MCNPX performs with respect to MPI (Message Pass Interface) and PVM (Parallel Virtual Machine) were conducted. PVM will no longer be supported by the LANL team after 2005, hence more emphasis is being put on how MCNPX runs with MPI on a Beowulf system.
- Parallelization factors that affect run times on a Beowulf system were run. Variables include criticality versus general transport, number of particles run per cycle, number of cycles, geometry concerns, material types, size of model environment, complexity of model environment, etc.

Oxygen Sensing in LBE (Task 13) Highlights:

- Members of the research group worked on the re-engineering of the newly built LBE pot system for testing the sensors in LANL.

- Several tests on heating device and oxygen control system (OCS) have been performed at LANL with the UNLV system.
- New numerical methods were applied to the 2-D simulation for the oxygen mixing in the apparatus.
- The 3-D simulation in FLUENT of the oxygen mixing was continued.

Positron Annihilation Spectroscopy (Task 14) Highlights:

- Residual stress measurements by neutron diffraction at the Atomic Energy of Canada Limited (AECL) have been analyzed.
- Residual stress measurements by the positron annihilation spectroscopy were conducted on different types of specimens at the Idaho Accelerator Center of ISU.
- Additional residual stress measurements by ring-core method will be performed next quarter at the Lambda Research Laboratory.
- Sample preparations are in progress to characterize imperfections/dislocations due to plastic deformation and welding by TEM.

1.3.3 Student Research Technical Summary

FUELS TECHNOLOGY

Remote Fuel Fabrication (Task 9). The hot cell robot kinematics were analyzed further. The trajectories of robotic manipulators can be planned in two ways: joint space and operational space. The joint space guarantees a smooth path for the joint angles, but does not guarantee a smooth profile of the end effector. For both planning methods, a 7^{th} order polynomial is used to generate the paths. Figure 1.3.1 shows a schematic of the trajectories used in the hot cell simulation:

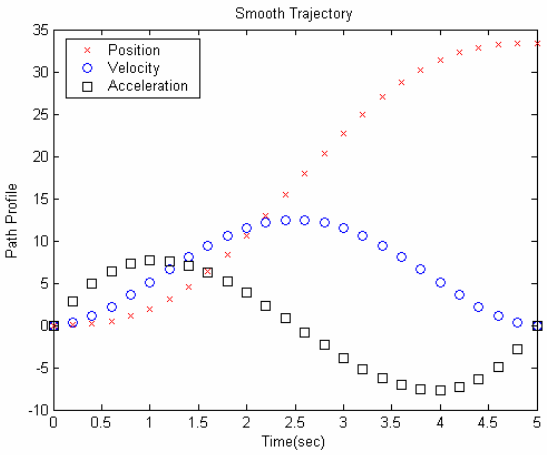

Figure 1.3.1. Smooth trajectories for joint angles and operational variables

Currently, a blend of joint space planning and operational space planning is used:

- Joint space planning methods are used when the manipulator is not holding any pellet. Trajectories produced by this method are easier to handle with the controller.

- Operational space methods are used whenever the pellets are being held by the manipulator. The scheme used is the famous pick-place scheme, where the end effector approaches the pellet, lifts up to some safety margin in order to avoid obstacles, then moves the object finally dropping it. This path planning method insures that the smooth motion profile of the end effector, and consequently of the pellet. The inverse kinematics is performed at a selected number of points of the path, and the joint angles found are used in the control scheme described above.

A grinder was added to the hot cell design. The grinder is basically a sloped trough, with two grinding wheels rotating on the sides. The whole trough vibrates, to assist the pellets in dropping into a tray. After the pellets are grinded, they are dropped into an output tray, from where they are loaded onto the V-tray for insertion into the cladding tube.

Further refinements were made to the object recognition tools developed by Dr. J.K. Lee. The focus was on improved segmentation and adaptive filtering for contour detection in CCD images.

SEPARATIONS TECHNOLOGY

Immobilization of Fission Iodine (Task 15). The recovery of iodine released during the processing of used nuclear fuel poses a significant challenge to the transmutation of radioactive iodine. This project examines the use of Fullerene Containing Carbon (FCC) compounds as potential sorbents for iodine release from the reprocessing of nuclear fuel. The experimental capability is also used to test other potential sorption materials and processes, such as natural organic matter (NOM) and other promising alternatives. This project also examines the development of a process to convert the sorbed iodine into a ceramic material with the potential for use as either a transmutation target or as a waste form in a partitioning and sequestration strategy.

The development of analytical methods for measuring the speciation of iodine under vapor and aqueous conditions are continuing. Pyrolysis is used to examine iodine release from NOM. Experiments with iodinated sphagnum moss were continued and the amount of iodine released as methyl iodide during pyrolysis has been quantified.

In order to address the formation of volatile and semi-volatile iodo-compounds, NOM solutions were exposed to iodine (at several pHs) and then the mixture was fractionated. The aqueous phase from these reaction mixtures was examined for semi-volatile species. Previous observations indicated only minute formation of iodoform and other volatile iodinated alkanes were formed. The formation of any semi-volatile organic iodides under these conditions was not detectable.

A second series of experiments was conducted where 0.5 g of unbuffered sphagnum was treated with 1.5 to 6.0 mL of 250 ppm iodine. After 24 hours of exposure the samples were dried and pyrolyzed *without the leaching procedure outline above*. The results indicated that more than 40% of the applied iodine was converted to methyl iodide. There was no indication of iodine dose dependence in the methyl iodide yield in these experiments, which was certainly surprising. However, the methyl iodide formed was 20-25 times the apparent blank levels and so

unambiguously related to the treatment. Iodine rich particles of sphagnum may be selectively sampled, for pyrolysis, because of differences in texture and density induced by the treatment.

Solution phase iodine binding experiments were conducted at various pHs with model organic compounds. Vanillin reacts with iodine at all pHs. However, at high pH the vanillin reduces I_2 to I^-, without incorporating any iodine into the aromatic ring. Under these conditions the reaction produces vanillic acid instead of iodovanillin. At all pHs the reaction kinetics are extremely rapid. In the presence of excess iodine the reaction is complete in less than 30 seconds (at pH 4-12). The rate of reaction is slower at pHs less than 3. Other model NOM compounds such as gallic acid and tannic acid have been examined. Both of these materials may be components of NOM and are therefore relevant model compounds. Both gallic and tannic acid reduce iodide to iodide exclusively with no covalent C-I bond formation. The effects of pH on the reaction of iodine with vanillin are presented in Figure 1.3.2.

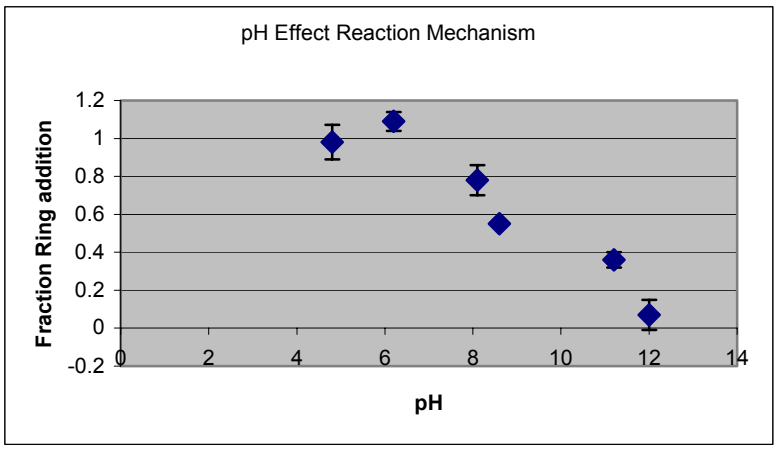

Figure 1.3.2. Fraction of iodine adding to aromatic ring in vanillin reaction. Reaction carried out with excess vanillin.

Additional experiments with the iodine generator and the fuel rod dissolution simulator have been conducted in order to examine the effects of nitric acid fumes and NOx (at 40°C) on iodine sequestration. Previously NOM traps, prepared with sphagnum peat and $Ca(OH)_2$, were able to trap iodine vapor in the presence of nitric acid vapor. Only a small fraction of the iodine was released by water leaching as iodide or iodate (<10%). If the main reaction was addition of iodine to the aromatic ring one iodide should be produced for each reacted iodine. The iodide should be leachable from the column. In the absence of nitric acid fumes, less than 15% of the adsorbed iodine was desorbed from the column with water. This is significantly less than the 50% predicted if addition to aromatic rings were the primary reaction. It is interesting to compare this result with the reaction of a suspension of sphagnum moss with an aqueous solution of iodine. At high pH (~12) about 30% of the iodide is converted to iodide in solution. At pHs of 5.7 most of the iodine was apparently reduced to iodide. The difference in behavior between gas phase sequestration and the solution reaction is puzzling and is under continuing investigation. Experiments with the fuel rod dissolution simulator indicate that both FCC and NOM are capable of trapping iodine.

Many of the trapping experiments used KI solution to rinse trapped "iodine" from the columns. The purpose of the KI solution was to convert trapped I_2 to I_3^-. It was observed that with the fuel rod simulations that the eluted iodine exceeded the starting material. It is known that nitric acid can oxidize iodide to higher oxidation states. Experiments with concentrated nitric acid and KI indicated rapid formation of I_2. Because significant quantities of nitrate and nitrite are measurable in both the bisulfite solutions and in aqueous extracts of the NOM and FCC traps we believe that KI was being oxidized by the nitric acid fumes thus creating the artifact. Buffering the KI solution with sodium bicarbonate subsequently eliminated this artifact. Because nitric acid can apparently oxidize iodide, speciation of iodine on the trap materials was examined. A number of experiments to determine the speciation of trapped iodine on FCC and NOM were performed. These experiments involved rinsing the trapping media with distilled water, which was subsequently analyzed by ion chromatography. Ion chromatography indicates that a significant amount of iodine trapped by FCC is converted to iodate. In the case of FCC 50-60% of the iodine could be desorbed as iodate. For NOM 20-30 % of the iodide was converted to iodate during simulation of fuel rod dissolution. In the presence of NOx the 50-60% was converted to iodate. Experiments were repeated with the iodine generator to see if iodate was formed during these experiments. Ion chromatography indicated that iodate formation of NOM was not significant under these conditions. Using the iodine generator 3-4 mg of iodine is transferred to the trap over 1-2 hours. In the case of the fuel rod simulation all of the iodine is placed in the flask where the dissolution process is simulated by warming and addition of Cu. It may be that this second procedure results in more rapid transfer of iodine from the system and increases the importance of oxidative side reactions.

The generation of NOx by the addition of copper metal may have some important consequences for iodine speciation. Results indicate that NOx oxidized trapped iodine on the FCC material to IO_3^-. The iodate was easily leached from the column by a water wash (and detected by ion chromatography). Rinsing the column with KI resulted in the generation of an equivalent quantity of I_2. Significant iodate was also produced by the NOM under these reaction conditions.

The formation of iodate has important implications for iodide binding by FCC material. NOx generation also complicates the determination of breakthrough volumes for iodine in the fuel rod dissolution simulator. NOx gas fills the reaction vessel and reacts with the bisulfite trapping solution. This limits the time available for monitoring breakthrough. In addition, the NOx oxidizes iodine that has been previously trapped by the bisulfite.

The transfer of iodide (in the form of KI) was examined in the fuel rod simulator experiments. It was believed that iodide released from fuel rods could be transferred from the sparging vessel as HI or some other volatile form of iodine. These experiments were conducted without out a solid phase absorbent in order to focus on the possible volatile forms of iodine created from KI and nitric acid. Iodine transfer was quantified by examining the composition of the bisulfite trapping solution. One possibility is that I^- could be oxidized to I_2 by the nitric acid, which would subsequently be sparged from the system. Other possible volatile forms of iodide are NOI (nitrosyl iodide) which were believed may be formed under these conditions. Several experiments were conducted with KI and nitric acid. Transfer rates were generally less than 25

% over 90 minutes of sparging. In the presence of NOx (Cu experiments) I^- was oxidized to iodate (in the reaction vessel). NOx carried over to the trapping solution depleted the bisulfate concentration. After one experiment conducted with 8 mg of KI, 500 mg of Cu in 25 mL of concentrated nitric acid, it was noted that the bisulfite trap took on a iodine like color. The trap solution reacted positively to KI starch paper indicated that I_2 was probably present in the solution. In order to confirm the presence of iodine, a known quantity of N,N-dimethyl aniline was added. This compound reacts quickly with molecular iodine to form 4-iodo-N,N-dimethyl aniline. The solution was extracted and complete iodinization was confirmed by GC/MS. The same experiment was conducted in the absence of copper. Without the NOx generation active iodine was not observed in the bisulfite trap. Apparently the NOx acts to deplete bisulfite and oxidize any iodide present to a "reactive" form (I_2, IOH, NOI). NOx likely contributes to oxidation of iodine on FCC and NOM traps as well.

From the work concluded so far, it is believed that iodine reacts with the NOM/$Ca(OH)_2$ by several mechanisms: Ring addition reactions, Reduction to iodide, and Disproportionation in strong alkali ($Ca(OH)_2$). It is believed that FCC adsorbs iodine as molecular iodine and thermal or chemical desorption from this material is facile.

The presence of NOx and nitric acid in these experiments has several effects. Both reagents are capable of oxidizing iodide. This may occur in the reaction vessel during the dissolution of fuel rods or after transfer to the FCC or NOM trap. The formation of highly water-soluble iodate would compromise the sequestration of iodine by either material.

TRANSMUTATION SCIENCES

Niobium Cavity Fabrication Optimization (Task 2).

Multipacting Studies: Multipacting studies have been replaced by secondary electron emission studies. The Monte Carlo Back Scattering and Secondary Electron Scattering code developed by Dr. David Joy (ORNL and University of Tennessee Knoxville) is being translated into C++ by a third student not associated with this research project. The purpose is to develop a more program friendly environment to modify the code and GUI (Graphics User Interface).

Experimental Set-up for the SEE from a Niobium Test Piece: A number of the experimental parts have arrived at UNLV and are being assembled and tested. Figure 1.3.3 shows a birds eye view of the current system with attached roughing pump, turbomolecular pump, and cryopump (not seen in figure) and residual gas analyzer diagnostic. Currently, the vacuum integrity of the chamber with components is being tested. The experimental system is still missing an electron gun. The gun is to arrive in the upcoming quarter. The electron position detector has arrived at UNLV. The gun and detector act as one unit and will be installed within the vacuum chamber in the near future. Half of the machined niobium samples have arrived. The remaining half should be here next quarter.

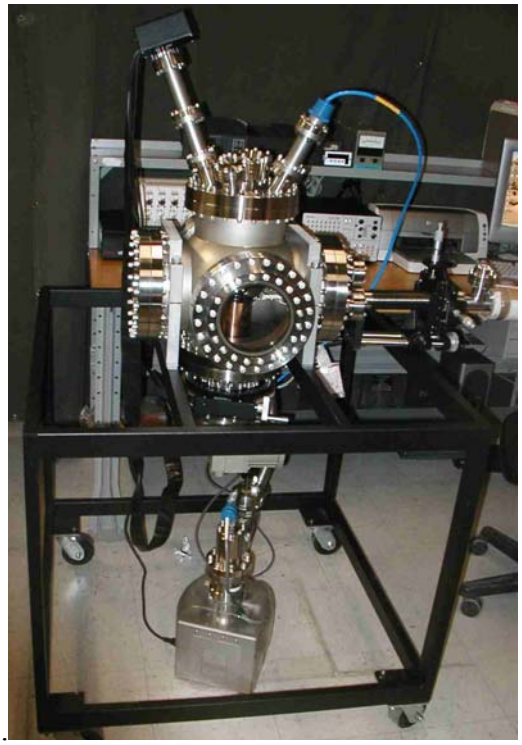

Figure 1.3.3. View of the experimental setup to date (3/26/04).

LBE Corrosion Modeling (Task 5). One of the critical obstacles to the wide use of LBE as a nuclear coolant is corrosion. Unprotected steel undergoes severe attack by liquid lead and lead-bismuth alloy by dissolution of its components in the liquid metal. The present study involves the estimation of corrosion in the liquid metal by imposing an analytically developed concentration expression on the wall surfaces and benchmarking the CFD tool and performing a series of parametric studies on the loop model. The concentration and temperature diffusions due to different flow regimes have been studied. Regions of maximal corrosion and precipitation have been deduced from the simulations and the results have been compared with the analytical models.

The first subtask of this project involves using a CFD code to obtain averaged values of stream wise velocity, temperature, oxygen and corrosion product concentrations at a location deemed close to the walls of the LBE loop at more than one axial location along it. The oxygen and corrosion product inside the test loop was simulated to participate in chemical reactions with the eutectic fluid as it diffuses through towards the walls.

The second subtask and the more important objective of this project is to use the information supplied by the first task as boundary conditions for the kinetic modeling of the corrosion process at the internal walls of the test loop. The outcome of the modeling will be fed back to the first subtask, and the steady state corrosion/precipitation in an oxygen controlled LBE system will be investigated through iterations. This should shed some light on the likely locations for corrosion and precipitation along the axial length of parts of the test loop.

Velocity, temperature and concentration profiles at four elbow regions of the Materials Testing Loop at LANL were modeled for laminar flow and turbulent flow this quarter. As anticipated for laminar flow, the inside edge of the sections of the elbow have higher dissemination rate than the outside edge. The effect of the secondary flows at the elbow sections and the consequent variation in the diffusivity justifies the peculiar trend of the corrosion/precipitation rate at the elbow sections.

It is noticeable that the temperature diffusion from the wall into the bulk of the fluid is not as significant for turbulent flow as it is for the case of a laminar flow. The higher velocities in the turbulent flow make the diffusion more predominant in the lateral direction than the transverse direction. The reasoning of the lower diffusion rate in the transverse direction than the lateral direction applies for the case of corrosion too. It was seen that the increase in velocity increases the corrosion rate and the decrease in velocity decreases the corrosion rate. This is true in the case of precipitation rate also, where the increase in velocity increases the precipitation rate.

3-D modeling in two pipe fitting geometries (a sudden expansion and a Tee section) was performed. These sections will be eventually placed in a LBE loop numerical simulation to find out how the concentration gradients develop inside these fittings. Vortex shedding was found to start to occur at Re = 1500 as indicated in Figure 1.3.4.

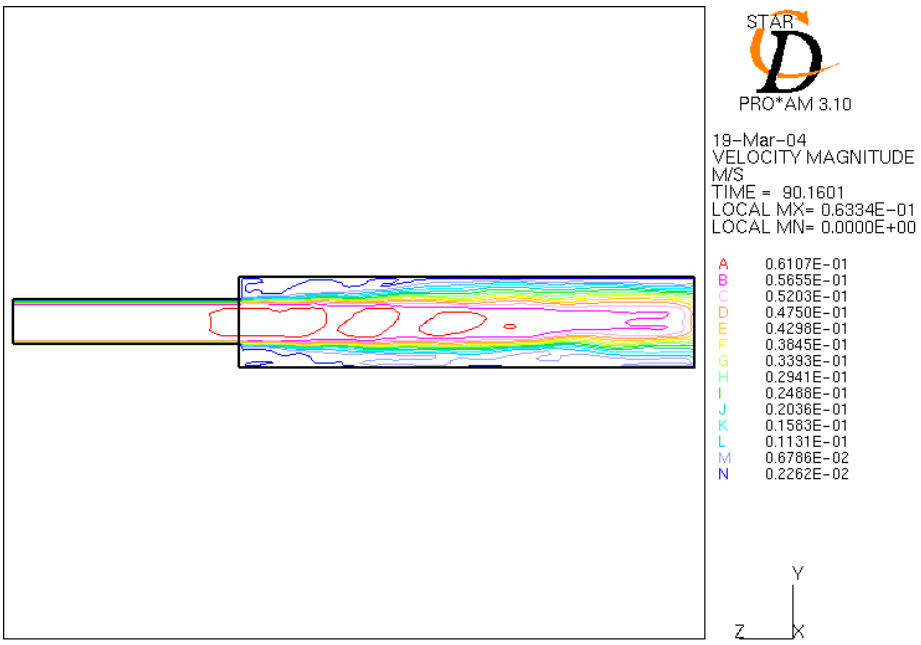

Figure 1.3.4. Velocity plot for Re = 1500

Some hydraulic studies regarding how diffusion, mass transfer and convection affect corrosion and precipitation rate of steel in oxygen controlled non-isothermal LBE loop piping system under various temperatures have been done. In these studies, it was assumed that chemical

reactions are much slower than the characteristic time of diffusion/convection and hence, they contribute little to the mass transfer in LBE bulk fluids.